CHARACTERIZATION AND EFFECTS OF HYDRIDES IN HIGH-BURNUP PWR CLADDING ALLOYS

M.C. Billone, T.A. Burtseva, and Y.Y. Liu

Argonne National Laboratory, 9700 South Cass Avenue, Lemont, IL 60439 USA, billone@anl.gov

In previous work conducted for the U.S. Nuclear Regulatory Commission (NRC) and the U.S. Department of Energy (DOE) Used Fuel Disposition Campaign, hydrogen content has been measured, hydride morphology and orientation have been characterized, and the effects of hydrides on ductility have been determined for cladding alloys from fuel rods irradiated to high-burnup (HBU) in commercial pressurized water reactors (PWRs). The PWR cladding alloys included Zircaloy-4 (Zry-4), ZIRLO™, and M5® in the as-irradiated condition and following simulated drying and storage at elevated temperature and pressure. The particular focus of this work was to determine the ductile-to-brittle transition temperature (DBTT) as a function of hydrogen content and peak drying-storage temperature, internal gas pressure, and pressure-induced hoop stress. Ring-compression tests (RCTs) were used to determine cladding ductility as a function of RCT test temperature, which in turn was used to determine DBTT. Characterization and RCT results from this work are summarized for HBU PWR cladding in the as-irradiated condition and following slow cooling from 400°C at peak hoop stresses in the range of 80 to 140 MPa. A direct correlation was found between 400°C hoop stress, the effective length of radial hydrides, and the DBTT. The radial-hydride continuity factor (RHCF) was used to determine the effective length of radial hydrides. Essentially, it is a measure of the fraction of cladding wall thickness along which unstable cracks can grow. While RHCF proved to correlate quite well with DBTT for HBU ZIRLO™ with 350 to 650 wppm hydrogen, a different relationship between DBTT and RHCF was found for M5® with only 60 to 90 wppm hydrogen. Other metrics were evaluated to determine the best metric or combination of metrics that correlated with DBTT for all PWR cladding alloys.

I. INTRODUCTION

Mechanical properties and failure limits are needed to assess fuel behavior during dry-cask storage, post-storage handling and transport, and post-transport handling. Normal conditions of transport (10CFR71.71) include free- and corner-drops of 0.3 m. Hypothetical accident conditions of transport (10CFR71.73) include a 9-m free drop. Handling accidents may result in intermediate drop distances. Pre-storage drying and transfer operations, as well as early stage storage, can subject cladding to higher temperatures and hoop stresses relative to in-reactor operation and pool storage. Under these conditions, radial hydrides may precipitate during slow cooling and provide an additional embrittlement mechanism as the cladding temperature decreases below the ductile-to-brittle transition temperature (DBTT).

Argonne has developed a test protocol and generated data for cladding from fuel rods irradiated to high burnup (HBU) in commercial PWRs. HBU Zircaloy-4 (Zry-4), M5®, and ZIRLO™ cladding alloys have been tested in the as-irradiated condition[1] and following simulated drying and storage[2-3] at the NRC-recommended peak temperature of 400°C (ISG-11, Rev. 3)[4] and at peak hoop stresses of 80 to 140 MPa. Experimentally, the protocol involves: (a) radial hydride treatment (RHT), during which high-burnup cladding is exposed to simulated drying-storage temperature and hoop stress conditions, including slow cooling and decreasing hoop stress, and (b) ring compression tests (RCTs), for which cladding rings are subjected to hoop bending stresses, to determine strength and ductility as functions of test temperature. Characterization, RCT, and DBTT data were documented in the IHLRWM-2013 proceedings[5] for as-irradiated cladding and cladding subjected to 400°C RHT hoop stresses of 110 and 140 MPa. These data are summarized, along with more recent data for PWR cladding alloys subjected to lower RHT stresses of 80 and 90 MPa.

Characterization data included hydrogen content, hydride morphology and orientation, and thicknesses of outer-surface oxide layer and the cladding metal wall. In particular, a radial-hydride metric was defined and used consistently throughout this work to correlate with DBTT. The radial-hydride continuity factor (RHCF), which is defined and justified in Ref. 2, is a measure of the effective fraction of the cladding wall thickness through which cracks can grow rapidly along continuous radial-circumferential hydrides. For HBU ZIRLO™ samples, which contained 350−650 wppm hydrogen, the DBTT decreased systematically from 185°C for 65% RHCF to

23°C for 19% RHCF to <20°C for <19% RHCF. However, for HBU M5® with 60−90 wppm hydrogen, the DBTT decreased from 80°C for 61% RHCF to <20°C for 37% RHCF. Also, as-irradiated HBU Zry-4 with >850 wppm of local circumferential hydrides was found to have a DBTT >90°C. These examples illustrate that the DBTT for HBU cladding depends on more than just the RHCF.

In the current work, other radial-hydride metrics are evaluated to determine how well they correlate with DBTT values measured for 350-wppm ZIRLO™ and for 60-wppm M5®. These metrics are: (a) radial-hydride number fraction $f_n(40°)$, where the number of hydrides within ±40° of the wall radius are normalized to the total number of hydrides, (b) radial-hydride length fraction $f_l(45°)$, where the total length of hydrides within ±45° of the radius is normalized to the total length of all hydrides, and (c) radial hydride length density RHLD, where the total length of hydrides within ±45° of the radius is normalized to the cladding cross sectional area.

II. MATERIALS AND TEST METHODS

II.A. Materials

TABLE 1 summarizes the HBU PWR cladding samples used in this study. The thermal mechanical treatment (TMT) of as-fabricated cladding alloys was found to be an important parameter. Recrystallized-annealed (RXA) M5® was more susceptible to precipitation of long radial hydrides than cold-worked and stress-relief-annealed (CWSRA) Zry-4 and ZIRLO™.

Burnup is an important parameter in determining the end-of-life rod internal pressure. However, cladding stress-strain properties and failure limits do not directly depend on fuel burnup. Rather, they depend on fast (>1 MeV) neutron fluence, hydrogen content (C_H), and hydride orientation. As can be seen in TABLE 1, C_H values vary from about 60 wppm to 650 wppm within a relatively narrow fuel-burnup range.

C_H values listed in TABLE 1 are based on measurements at three to five axial locations within about 45 mm and three to four arc segments at each axial location. The ± values represent the one-sigma variation in these measurements. For mean C_H values ≥350 wppm, the circumferential variation in hydrogen content is much larger than the axial variation.

Also listed in TABLE 1 are target RHT hoop stresses (σ_θ) for test samples, which were about 78 mm long cladding segments fabricated at room temperature (RT, 23°C) to form pressurized and sealed rodlets. The RT internal pressure was selected, along with estimates of cladding-metal outer diameter (D_{mo}) and wall thickness (h_m), to give the target hoop stress at 400°C. Actual hoop stresses were calculated following RHT based on oxide-layer thickness and h_m values measured from metallographic images.

TABLE 1. Summary of Cladding Materials and Target RHT Hoop Stresses at 400°C. AI is as-irradiated.

Cladding Alloy	TMT	Burnup, GWd/t	C_H, wppm	Target σ_θ, MPa
Zry-4	CWSRA	67	300±15	AI
			640±140	AI
			520±90	110
			615±82	140
M5®	RXA	70	76±5	AI
		68	58±15	90
		68	72±10	110
		63	94±4	140
ZIRLO™	CWSRA	68	530±70	AI
		68	535±50	80
		68	480±131	90
		68	530±100	90
		70	350±80	110
		70	425±63	110
		70	650±190	140

II.B Test Methods

II.B.1. Radial-Hydride Treatment

Pressurized and sealed rodlets were heated from 23°C to about 400°C, stabilized at 400°C with 0.17-MPa argon gas pressure external to the rodlet, held at 400°C for 1 to 24 h (reference hold time was 1 h), and cooled slowly at 5°C/h to either 200°C (high-C_H Zry-4 and ZIRLO™) or 130°C (low-C_H M5®), and then cooled more rapidly to RT. Pre- and post-RHT measurements were made to determine the outer-diameter (D_o) of the corroded cladding Based on previous results for Zr, Zry-2, and Zry-4,[6-8] the solubility limit is 206 wppm during the heating phase, and dissolution of hydrogen is very rapid. Thus, 206 wppm is predicted to dissolve in the Zry-4 and ZIRLO™ listed in TABLE 1, while all the hydrogen should be dissolved in the M5® samples used in this study. Unlike dissolution during heating, precipitation during cooling is a non-equilibrium phenomenon that requires hydrogen super saturation to precipitate new hydrides in the metal matrix. The initiation of new-hydride precipitation would occur at 335°C for samples with 206 wppm dissolved hydrogen at 400°C [7]. For low-C_H M5®, precipitation of hydrides would initiate at 245°C to 283°C for samples with 58 to 94 wppm dissolved hydrogen[8]. The precipitation temperature (T_P) determines the rodlet internal pressure and corresponding hoop stress relevant to the initiation of radial-hydride precipitation.

II.B.2. Ring Compression Testing

RCT loading induces hoop bending stresses, along with secondary axial stresses, due to the long ring length (≈8 mm)) relative to h_m (0.57 to 0.77 mm). Figure 1 shows the controlled displacement (δ) and the measured

load (P) at the 12 o'clock orientation. The maximum bending moment (M_{max}) occurs at the 12 and 6 o'clock positions, which induces maximum tensile hoop stresses [$(\sigma_\theta)_{max}$] and strains [$(\varepsilon_\theta)_{max}$] at the inner surfaces below the load and above the support. For cladding with radial hydrides emanating from the inner surfaces, crack initiation will likely occur at 12 and/or 6 o'clock. The bending moment at 3 and 6 o'clock, which is about 40% smaller, induces tensile hoop stresses and strains at the cladding outer surface. For cladding with radial hydrides emanating from the outer surface and/or for cladding with a hydride rim, crack initiation will likely occur at one or both of these locations.

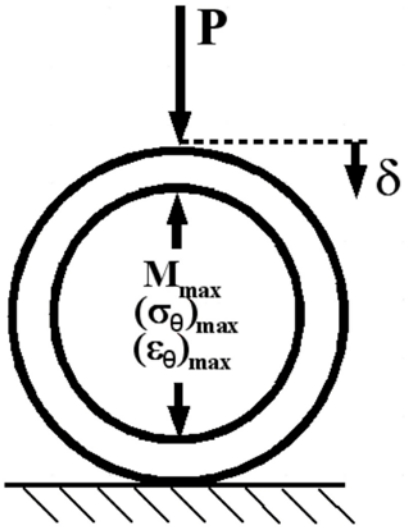

Fig. 1. RCT loading (P) and controlled displacement (δ).

RCTs were conducted at a controlled displacement rate of 5 mm/s to a maximum displacement of 1.7 mm. For as-irradiated HBU cladding, an increase in displacement rate from 0.05 mm/s to 50 mm/s had no significant effect on maximum load and ductility. The 1.7-mm displacement limit was chosen to give about 10% plastic deformation for rings that survived the RCT without cracking. Prior to conducting a RCT, the ring outer diameter (D_{oi}) was measured along the loading direction. The measurement was repeated after the RCT for rings that showed no evidence of cracking to give the post-test outer diameter (D_{of}) and the permanent displacement ($d_p = D_{oi} - D_{of}$). Permanent strain for the ring was calculated by normalizing d_p to D_{mo}. For HBU corroded cladding, the error in this approach is estimated to be <1% strain. Most of this error comes from delamination and spallation of the oxide layers under the loading plate and above the support plate. Rings which exhibited <1% permanent strain were classified as brittle. Accurate values for permanent strain can only be measured for rings that do not crack (e.g., as-fabricated cladding used for benchmark tests and low-C_H HBU M5®) and for slow-displacement-rate (e.g., 0.05 mm/s) RCTs for which the test can be terminated following the first significant load drop (>25%) indicative of a crack extending through >50% of the wall). For the fast-displacement-rate loading used in the current work, the measure of plastic displacement prior to >25% load drop is the offset displacement.

The traditional way to determine offset displacement (δ_p) is to mathematically unload the sample using the loading stiffness. However, the RCT unloading stiffness is always less than the loading stiffness[2-3]. Benchmark tests were conducted with as-fabricated cladding to determine that the unloading/loading stiffness ratio decreased linearly from 1 to 0.773 with the traditional offset strain (δ_p/D_{mo} in %) for $\delta_p/D_{mo} \leq 8.3\%$ and was 0.773 for δ_p/D_{mo} >8.3%. This relationship was used to correct offset strain determined from the load-displacement curves. For δ_p/D_{mo} (corrected) <2% prior to >25% fast load drop, samples were classified as brittle.

III. DBTT RESULTS FOR HBU PWR CLADDING

III.A. HBU Zry-4

TABLE 2 summarizes DBTT results for HBU Zry-4. Actual stresses at 400°C are listed. For 300-wppm Zry-4, the hydride rim was relatively thin and the sample survived 1.7 mm of RCT displacement at 5 mm/s and 20°C with no cracking. This demonstrated that the Zry-4 metal has relatively high RCT ductility even at 1.4×10^{26} n/m^2 fast-fluence level. However, for 640-wppm Zry-4 irradiated to the same fast fluence, the large circumferential variation in C_H resulted in regions of the cladding with >850 wppm C_H and a hydride rim that extended through >50% of the cladding wall. The material behaved in a brittle manner with cracking initiating at 3 and 9 o'clock outer-wall locations and propagating through 70% of the wall. Metallographic examination of the two RHT rodlets indicated that HBU Zry-4 had relatively low susceptibility to radial hydride precipitation. These relatively short radial hydrides participated in crack propagation, but they did not contribute to crack initiation at the cladding outer surface. Thus, HBU Zry-4 is more susceptible to embrittlement due to circumferential hydrides than to radial hydrides.

TABLE 2. Summary of Results for HBU Zry-4.

C_H, wppm	σ_θ(400°C), MPa	$\sigma_\theta(T_P)$, MPa	RHCF, %	DBTT, °C
300±15	AI	AI	0	<20
640±140	AI	AI	0	>90
520±90	114	103	9±5	<20
615±82	145	131	16±4	60

III.B. HBU M5®

TABLE 3 summarizes DBTT results for HBU M5®. As-irradiated HBU M5® exhibited high RCT ductility at 20°C for displacement rates of 0.05, 5, and 50 mm/s. No cracks were observed after 1.7-mm displacement. The estimated fast fluence for this material is 1.6×10^{26} n/m^2. HBU M5® exhibited high susceptibility to radial-hydride precipitation during RHT cooling at relatively low stress levels. This is indicated by the high RHCF values (includes results presented in Section IV for 58-wppm M5®) listed in TABLE 3. The relevant peak hoop stresses for radial-hydride precipitation were 69 MPa at 245°C (58 wppm C_H), 88 MPa at 261°C (72 wppm C_H), and 117 MPa at 283°C (94 wppm C_H). Many of the long radial hydrides emanated from the cladding outer surface into the cladding wall. Yet, the DBTT values were lower than anticipated based on the radial-hydride lengths. While the combination of RXA microstructure and low C_H makes HBU M5® more susceptible than HBU Zry-4 to precipitation of long radial hydrides, the low hydrogen content appears to make the material less susceptible to embrittlement. This issue is addressed in Section IV. Also, the decrease in RHCF from 61% to 54% to 37% occurred with the decrease in $\sigma_\theta(T_P)$ and the decrease in C_H. Without further testing, it is not clear if the decreases in RHCT and DBTT were due to the decrease in stress, the decrease in C_H, or a combination of the two.

TABLE 3. Summary of Results for HBU M5®.

C_H, wppm	σ_θ(400°C), MPa	$\sigma_\theta(T_P)$, MPa	RHCF, %	DBTT, °C
76±5	AI	AI	≈0	<20
58±15	90	69	37±17	<20
72±10	111	88	54±20	70
94±4	142	117	61±18	80

III.C. HBU ZIRLO™

TABLE 4 summarizes results for HBU ZIRLO™. As-irradiated ZIRLO™ used in this test program had a very dense hydride rim with a low density of hydrides below the rim. The primary difference between high-C_H (650 wppm) and low-C_H (350 wppm) ZIRLO™ was the average thickness of the outer-surface hydride rim. For some of the high-C_H samples, the circumferential variation in hydrogen was quite large. This corresponded to the observed variation (as much as a factor of two) in hydride rim thickness, which was likely due to circumferential variations in temperature for these fuel rods. Hydrides below the rim, particularly within the inner two thirds of the cladding, were sparsely distributed circumferential hydrides. C_H was ≈140 wppm (136±7 wppm) within the inner two-thirds of the cladding wall for the as-irradiated sample in TABLE 4.

TABLE 4. Summary of Results for HBU ZIRLO™.

C_H, wppm	σ_θ(400°C), MPa	$\sigma_\theta(T_P)$, MPa	RHCF, %	DBTT, °C
530±70	AI	AI	0	<20
535±50	80	72	9±3	<20
480±131	88	80	20±9	23
530±100	89	80	19±9	23
350±80	112	101	32±13	122
425±63	112	101	27±10	<150
650±190	141	128	65±17	185

For as-irradiated HBU ZIRLO™, the RCT ductility was about 7% at 20°C (independent of displacement rate). This demonstrated that the metal below the hydride rim deformed plastically before cracks through the hydride rim initiated and propagated through >50% of the cladding wall. As the RCT temperature was increased from 20°C to 90°C to 150°C, the RCT ductility increased from 7% to 11% and the number of cracks and average crack depth through the hydride rim into the cladding metal decreased with increasing test temperature.

For pressurized rodlets subjected to RHT, the RHCF and DBTT increased in a consistent manner with increasing RHT hoop stress. Figure 2 shows the increase in DBTT with RHT hoop stress. The solid points show the hoop stresses at 400°C while the hollow points are based on the hoop stress at T_P (335°C). The sample with the highest C_H (650 wppm) and RHCF (65%) had about 5% ductility at 195°C. This indicates that the relationship between DBTT and RHT hoop stress should be nonlinear with a decreasing effect of radial hydrides on DBTT as the test temperature approaches 200°C.

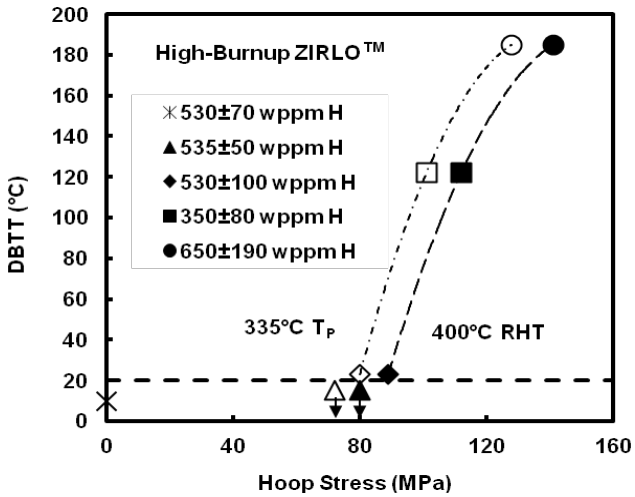

Fig. 2. DBTT as a function of 400°C RHT hoop stress (solid symbols) and hoop stress at 335°C (open symbols).

Figure 3 shows the increase in DBTT with increasing RHCF. The RCT databases for about 32% and 20% RHCF are reasonably robust (8 data points per RHCF).

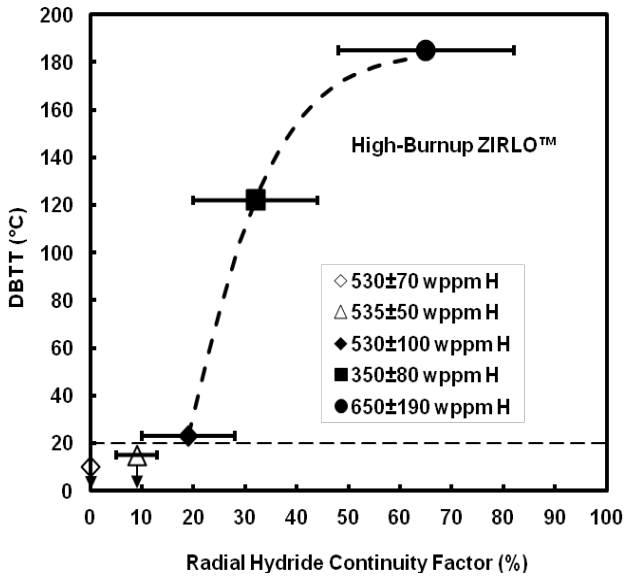

Fig. 3. DBTT as a function of RHCF for HBU ZIRLO™.

However, no data are available for DBTT values between 23°C and 122°C. This data gap corresponds to 400°C hoop stresses in the range of about 90 to 110 MPa and precipitation hoop stresses in the range of about 80 to 100 MPa.

IV. RADIAL HYDRIDE METRICS

Although the database for DBTT vs. RHCF is relatively sparse (3 data points for DBTT ±123°C), the results indicate that the DBTT for HBU ZIRLO™ correlates reasonably well with the RHCF metric. However, the same correlation does not apply to HBU Zry-4 and M5®. For HBU Zry-4, embrittlement appears to be a strong function of total hydrogen content and the pre-RHT distribution of hydrides across the cladding wall. For HBU M5® with only 60 to 90 wppm C_H, lower DBTT values were determined for higher RHCF values relative to HBU ZIRLO™. These results indicate that RHCF alone is insufficient to predict the DBTT for all PWR cladding alloys with a wide range of C_H values.

In order to address this issue, ZIRLO™ and M5® metallographic samples with comparable RHCF values (33% to 36%) and large differences in DBTT values (122°C vs. <20°C) were chosen for re-imaging to cover 100% of the cross sections, re-evaluation to better determine RHCF values, and evaluation to determine other metrics that have been used to characterize radial hydrides. Prior to re-imaging, the samples were carefully re-ground, re-polished, and re-etched to avoid possible over-etching of the ZIRLO™ sample and possible under-etching of the M5® sample.

The selected samples were from an HBU ZIRLO™ rodlet (648C) subjected to a 400°C RHT hoop stress of 112 MPa prior to cooling and from an HBU M5® rodlet (651E3) subjected to a 400°C RHT hoop stress of 90 MPa prior to cooling. C_H values for these rodlets were 350±80 wppm and 58±15 wppm, respectively. The specific ID numbers for the metallographic samples were 648C7 (pre-RCT) and 651E3D1 (post-RCT), respectively.

Previously published[2,9] metallographic images of the ZIRLO™ 648C7 surface suggested that the sample was somewhat over-etched based on the large width of the hydrides. Extensive re-grinding (about 0.1 to 0.2 mm) of the surface was required to remove previously etched material. This experience suggested that the original sample was over-etched and that there was good continuity of radial-hydride platelets in the axial direction. For the M5® 651E3D1 surface, only light grinding was required to remove all traces of the previous etching. This could be due to slight under-etching of the previous sample and/or poor continuity of hydride platelets in the axial direction.

IV.A. Images for HBU ZIRLO™ Sample 648C7

Metallographic images were obtained at 100X, 200X, and 500X magnification. The 100X images were taken at 36 circumferential locations to ensure coverage of the whole cross section. The 200X and 500X images were taken at selected locations with interesting arrays of radial hydrides. Figure 4 shows relatively long radial hydrides at the 4:30 o'clock position. The radial hydride labeled P1 has a projected continuous length of 50% of the wall thickness. If the P1 hydride were located at the 12 or 6 o'clock RCT location, a rapid load drop of ≈25% of corresponding to a 50% wall crack, would occur prior to plastic deformation for T <DBTT. The hydride labeled P2 is shorter (40% projected length), but its continuous projected length depends on the degree of continuity along the adjoining circumferential hydride connected to the next radial hydride. In Fig. 4, there is a discontinuity at ≈90 μm along the circumferential hydride.

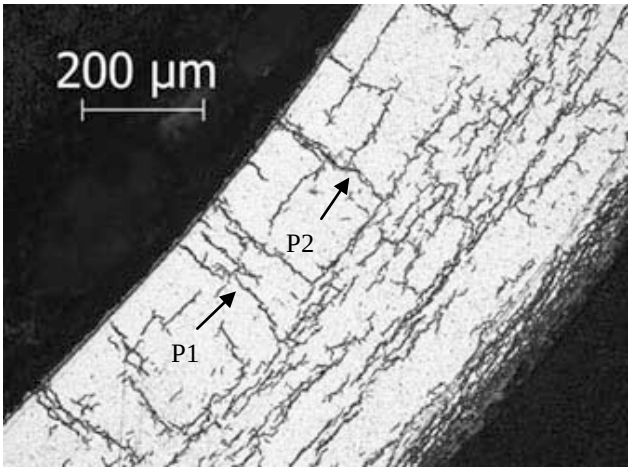

Fig. 4. 100X image of HBU ZIRLO™ sample 648C7 at the 4:30 o'clock orientation.

Higher magnification imaging was used to investigate the degree of continuity for the P2 radial hydride shown in Fig. 4. Figure 5 shows a 200X image of the location containing the P2 hydride. The gap indicated by the arrow appears to be narrower in the 200X image. If crack initiation occurred at the inner-surface hydride tip, rapid crack propagation through≈40% of the wall would occur followed by more stable crack growth along 90 μm of the circumferential hydride. If the crack grew to the next radial hydride, it could propagate further into the wall. With continued RCT displacement, the crack could propagate in stages as much as 75% into the cladding wall. Figure 6 shows the 500X image of radial hydride P2. There appears to be small gaps along the radial hydride. However, these gaps are probably too small to impede rapid crack growth.

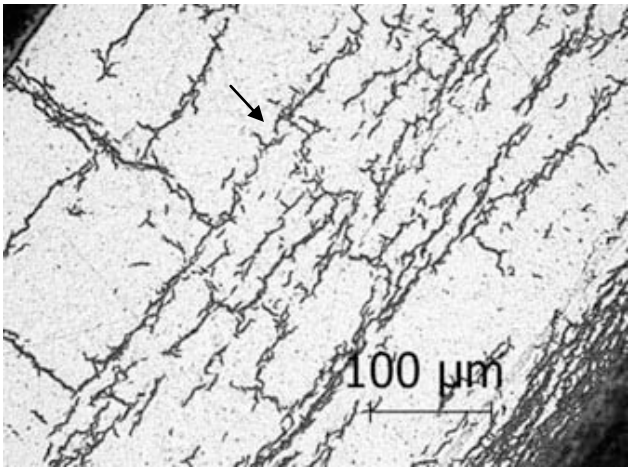

Fig. 5. 200X image of HBU ZIRLO™ sample 648C7 at the 4:30 o'clock orientation.

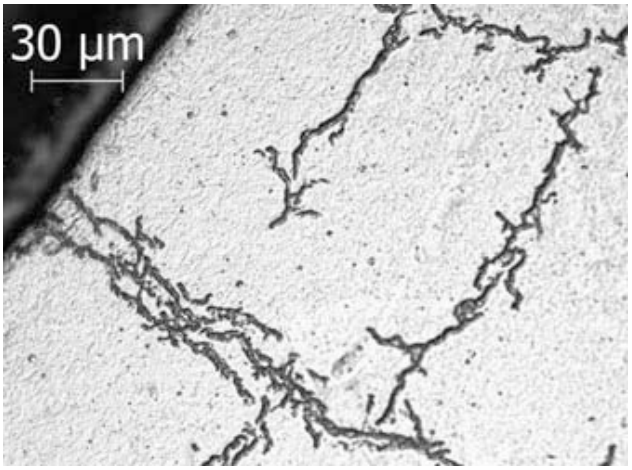

Fig. 6. 500X image of HBU ZIRLO™ sample 648C7 at the 4:30 o'clock orientation.

Figures 4−6 indicate that some judgment is involved in the interpretation of the effective lengths of radial hydrides for potential crack-growth paths.

IV.B. Images for HBU M5® Sample 651E3D1

In parallel with the work performed for the ZIRLO™ sample, 100X images were taken at 37 locations to cover the whole cross section and to allow some overlap between the images for identification of specific radial hydrides. Figure 7 shows the 100X image at the 10 o'clock orientation, which contained the longest radial hydride with a projected length along the radius of 73%. Based on this image, the radial hydride appears to be continuous and to emanate from the cladding outer surface. The 200X image shown in Fig. 8 indicates that the hydride has small regions of discontinuity, particularly near the tip of the hydride. The 500X image in Fig. 9 gives a better view of the discontinuity near the tip of the radial hydride. If this hydride were located at the 3 or 9 o'clock RCT orientation, a crack could initiate and grow through >50% of the cladding wall and perhaps as much as 73% of the cladding wall.

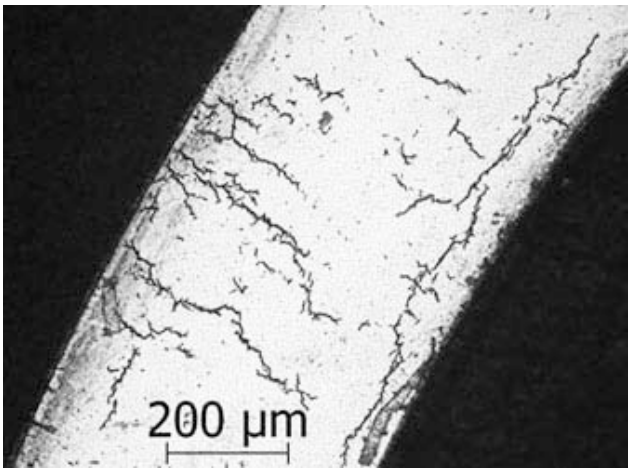

Fig. 7. 100X image of HBU M5® sample 651E3D1 at the 10 o'clock location.

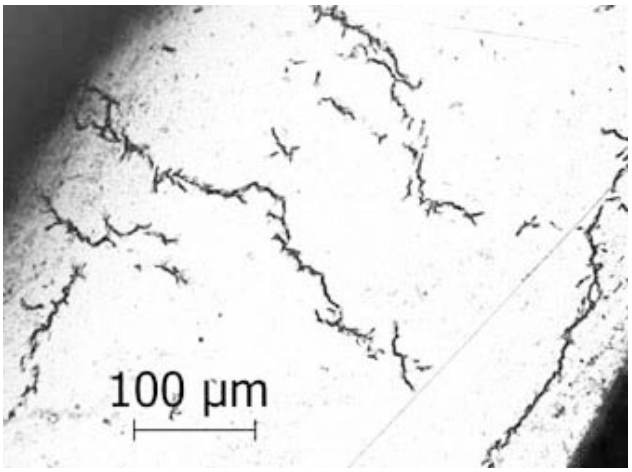

Fig. 8. 200X image of HBU M5® sample 651E3D1 at the 10 o'clock location.

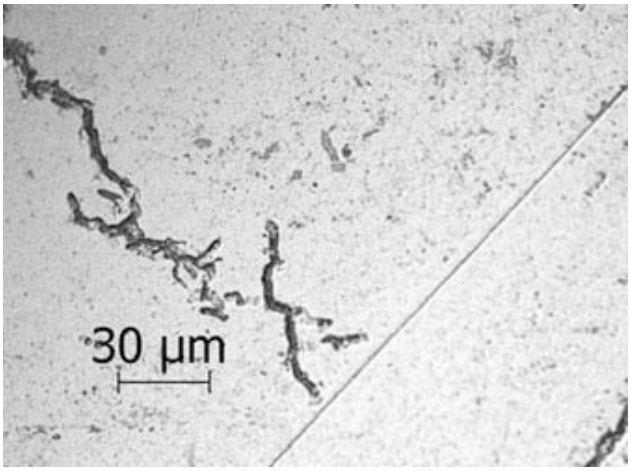

Fig. 9. 500X image of HBU M5® sample 651E3D1 at the 10 o'clock location.

IV.C. Evaluation of Radial Hydride Metrics

Aomi et al.[10] give a detailed description of the metrics $f_n(40°)$ and $f_l(45°)$. The metric $f_n(40°)$ is useful for assessing cladding microstructure, but it not predictive of cladding embrittlement or DBTT. The metric $f_l(45°)$ is also unlikely to correlate with DBTT. However, as it is commonly reported in the literature, it is determined in the current work. It is also redefined as radial hydride fraction [RHF = $f_l(45°)$]. RHF and RHLD are evaluated in the following subsections. RHCF is re-evaluated based on the additional data metallographic data.

IV.C.1. Radial Hydride Fraction (RHF)

RHF is the ratio of the total length of hydrides oriented within ±45° of the radius normalized to the total length of all hydrides. Short hydrides (<16 µm in length) are commonly ignored in this calculation. RHF has no significant meaning within the dense hydride rim of ZIRLO™. The circumferential hydrides are so densely packed that RHF is essentially zero for this region. As such, the rim region was excluded from determination of RHF, and emphasis was placed on the inner two-thirds of the cladding wall for ZIRLO™. On the basis of 36 images for ZIRLO™ sample 648C7, RHF = 0.30±0.05, where the 0.05 represents one standard deviation in the measurements. Based on the 37 images for M5® sample 651E3D1, RHF = 0.81±0.08. Given that the DBTT for the ZIRLO™ rodlet 648C was 123°C and the DBTT for the M5® 651E3D rodlet was <20°C, there appears to be no correlation between RHF and DBTT for these materials.

IV.C.2. Radial Hydride Length Density (RHLD)

RHLD is the ratio of the total length of hydrides oriented within ±45° of the radius normalized to the cross sectional area examined. Short hydrides (<16 µm in length) are commonly ignored in this calculation. As with the determination of RHF, the hydride rim in ZIRLO™ cladding was ignored. Based on the same set of images used to determine RHF, the RHLD values determined for HBU ZIRLO™ and M5® images were 7.47±1.68 mm^{-1} and 5.84±1.36 mm^{-1}, respectively. Thus, RHLD correlates better with the DBTT of these two alloys than does RHF. However, it is not clear it discriminates well enough with to rationalize >120°C difference in DBTT between the two alloys.

IV.C.3. Radial Hydride Continuity Factor (RHCF)

Based on the original set of 33 100X images for HBU ZIRLO™ sample 648C7, the RHCF was determined to be 33±14%. For the new 36 images, the RHCF was essentially the same (32±12%). The consistency of these values suggests good axial continuity of radial hydride platelets within 0.1 to 0.2 mm. Combining these two sets of measurements gives 32±13% RHCF

The previous RHCF value for HBU M5® sample 651E3D1 was 36±14% based on 100X images at 21 locations. The RHCF determined from the new 37 images was significantly higher (47±16%). Measurements at other axial locations of rodlet 651E3 gave 24±9% based on 100X images at 20 locations and 33±19% based on 100X images at 15 locations. The combined results for rodlet 651E3 were 37±15%. The axial variation from 24% to 47% suggests that continuity of radial hydride platelets may be poor in the axial direction for low-C_H M5®, especially for this particular rodlet with only 58±15 wppm C_H.

IV.C.4. Additional Data for RHLD and RHCF

There is another factor to be considered in evaluating the effectiveness of radial-hydride metric in predicting DBTT. RCT loading induces hoop bending stresses that are tensile at 12 and 6 o'clock inner surfaces and the 3 and 9 o'clock outer surfaces. These stresses transition from tensile at the indicated surfaces to essentially zero at the cladding mid-wall location to compressive at the opposite surfaces. Therefore, the location of radial hydrides is important to the mechanical response of RCT samples. Radial hydrides that emanate from the inner cladding surface are the most damaging. Radial hydrides that emanate from the outer cladding surface are less damaging because the bending moment at the 3 and 9 o'clock locations is about 40% less than the bending moment at the 12 and 6 o'clock locations. Radial hydrides near the cladding mid-radius are essentially benign with regard to crack initiation. This suggests that RHLD and RHCF should be determined for the inner-, middle- and outer-regions of the cladding wall (excluding the hydride rim). A weighting factor should be used to combine these values. Also, radial hydrides that emanate from the inner or outer surfaces should have higher weighting factors than internal radial hydrides.

In order to explore the effect of radial-hydride location within the cladding, the RHLD was determined for the inner-third, middle-third, and outer-third of the cladding wall for the two surfaces of interest. Based on wall averaged values presented earlier, the RHLD ratio for ZIRLO™ relative to M5® was 1.28. The ratios for inner-third, middle-third, and outer-third of the cladding wall were 1.77, 1.25, and 0.88. The inner-third-wall ratio of 1.77 ratio would be more discriminating than the average ratio of 1.28.

With regard to the RHCF, the longest radial hydrides for the ZIRLO™ cross section contacted the inner cladding wall at 24 out of 36 locations. The longest radial hydrides for the M5® section imaged emanated from the inner surface of the cladding at 7 locations and emanated from the outer surface at 8 locations. At the remaining 22 locations, the long radial hydrides did not extend to either surface. These results suggest that radial hydrides in the ZIRLO™ rodlet 648C should be more damaging than the radial hydrides in the M5® 651E3D1 rodlet. It requires less applied energy (or stress) to initiate a crack at the cladding surface than it does to initiate and internal crack.

V. DISCUSSION

V.A. DBTT Database and Cladding Failure Limits

The RCT database generated for the DBTT of PWR cladding alloys is more of a scoping database than a robust database. Even within the context of a scoping database, there are "holes" that should be filled for the three HBU PWR alloys tested in the as-irradiated condition and following simulated drying and storage (RHT). Also, to make the database more robust, repeat RHT tests should be conducted, followed by RCTs in a narrow temperature range to determine data scatter. The additional scoping tests that should be conducted are highlighted below.

For the HBU 15×15 Zry-4 cladding tested in this program, embrittlement due to circumferential hydrides occurred at≤90 °C for material with 640±140 wppm hydrogen. The peak hydrogen content measured for quarter rings was 850 wppm. Results from metallographic examination indicated that the peak local C_H across the cladding wall was >850 wppm. Additional data are needed for such samples at >90°C to determine the DBTT for HBU Zry-4 with high C_H. Samples with lower hydrogen content (e.g., 615±82 wppm with 715-wppm peak measured hydrogen content) had lower DBTT values (e.g., 60°C) following RHT than the as-irradiated samples. With regard to radial-hydride-induced embrittlement, the short radial hydrides precipitated in Zry-4 at RHT stresses as high as 145 MPa at 400°C did not contribute to crack initiation, although they did participate in crack propagation.

For the HBU 17×17 M5® tested in this program, hydrogen contents were low and coincidently decreased from rodlet to rodlet as the 400°C RHT hoop stress decreased. It is not clear if the decrease in DBTT was due to the decrease in stress (142 to 111 to 90 MPa) or the decrease in hydrogen content (94 to 72 to 58 wppm) or a combination of the two factors. Additional tests should be conducted at 400°C RHT hoop stress of 100 MPa for rodlets with about 90 wppm hydrogen. As all hydrogen in M5® dissolves at≥330 °C for ≤94 wppm hydrogen, these tests can also be conducted at peak RHT conditions of 350°C (considered to be a more representative peak cladding temperature) and 92-MPa hoop stress.

The DBTT database for the HBU 17×17 ZIRLO™ used in this test program is more extensive than the databases generated for the other two PWR cladding alloys. The 23°C DBTT for peak RHT conditions of 400°C and about 90 MPa is based on RCTs (2 at each temperature) conducted at RT, 60°C, 90°C, and 120°C. The 122°C DBTT for peak RHT conditions of 400°C and 112-MPa hoop stress is based on four RCT data points at 150°C, one RCT data point at each temperature of 120°C, 90°C and 60°C, and two RCT data points at RT. However, no data are available for DBTTs >23°C and <122°C. Additional tests should be conducted at peak RHT conditions of 95 to 105 MPa at 400°C and/or 87 to 97 MPa at 350°C.

It is quite likely that as-irradiated HBU Zry-4 and ZIRLO™ would have exhibited the same degree of embrittlement for the same distribution of hydrides across the cladding wall. The highly dense and concentrated hydride rim in ZIRLO™ and the more diffuse hydride rim in HBU Zry-4 likely resulted from differences in operating conditions (e.g., higher time-averaged heat flux at the cladding inner surface for ZIRLO™) than from differences in materials. The as-irradiated hydride distribution across the cladding wall may have also influenced the susceptibility of these materials to radial hydride precipitation. However, other researchers[10] have observed the same high susceptibility of ZIRLO™ relative to Zry-4 for materials with comparable distributions of hydrides across the cladding wall.

RCTs give load vs. displacement data for cladding rings without fuel inside. Higher failure loads are anticipated for fueled cladding. However, the RCT load vs. displacement data can be converted to stress and strain vs. displacement by inputting axial and hoop tensile properties into a finite-element code Argonne has developed to model RCT loading. Axial tensile properties can be measured for sibling samples at the same fast-fluence level. An iterative approach has been developed and benchmarked to determine the hoop tensile properties, as well as failure stresses and strains, based on matching the code predictions to the measured RCT load vs. displacement curves.

V.B. Radial Hydride Metrics

Three radial hydride metrics were measured for new metallographic images and evaluated with respect to DBTT data: radial-hydride fraction (RHF), radial-hydride length density (RHLD), and radial-hydride continuity factor (RHCF). The objective of this exercise was to find a metric or combination of metrics that would trend with measured DBTT values: 123°C for HBU ZIRLO™ with about 350 wppm hydrogen and <20°C for HBU M5® with about 60 wppm hydrogen. It was previously established that there was a good correlation between RHCF and DBTT for HBU ZIRLO™. However, higher RHCF values correlated with lower DBTT values for HBU M5®.

The RHF commonly reported in the literature exhibited the opposite trend with respect to measured DBTT values: low for HBU ZIRLO™ with 123°C DBTT and high for HBU M5® with <20°C DBTT. This metric is not recommended as a predictor of DBTT.

The RHLD trended with DBTT: higher for HBU ZIRLO™ and lower for HBU M5®. However the increase for ZIRLO™ relative to M5® was only 30% and may not be enough of an increase to rationalize the differences in DBTT values. The difference (77%) was more significant for RHCF evaluated for the inner-third of the cladding wall where radial hydrides are most damaging. While promising, this metric has not yet been evaluated for ZIRLO™ subjected to a range of peak RHT stresses from 80 to 140 MPa.

New results for the RHCF were combined with previous results. RHCF values for ZIRLO™ remained comparable to those for M5® even though there was a significant difference in DBTT values. Results were more promising if the RHCF were determined in such a way that radial hydrides emanating from the inner cladding surface were weighted higher than radial hydrides emanating from the outer cladding surface.

The radial hydride metrics comparison indicated that both RHLD and RHCF (or a combination of the two) could be used to predict DBTT if the locations of radial hydrides across the cladding wall were taken into account. However, additional data are needed for M5® with >90 wppm to evaluate the effects of axial continuity of radial hydrides on the DBTT.

In summary, RHCF correlated quite well with DBTT for HBU ZIRLO™ test materials with 350 wppm to 650 wppm C_H, dense hydride rims, and relatively low CH (about 140 wppm) below the hydride rims. The relationship established between RHCF and DBTT for this ZIRLO™ material, however, is not universal. HBU M5® exhibited lower DBTT values for higher RHCF values. HBU Zry-4, with a diffuse hydride rim and high CH exhibited embrittlement and >90°C DBTT for 0% RHCF.

ACKNOWLEDGMENTS

This research was performed at Argonne National Laboratory and supported by the Used Fuel Disposition Research and Development, Office of Nuclear Energy (NE-53) under Contract DE-AC02-06CH11357.

REFERENCES

1. M.C. Billone, T.A. Burtseva, and Y.Y. Liu, *Baseline Studies for Ring Compression Testing of High-Burnup Fuel Cladding*, FCRD-USED-2013-000040 (ANL 12/58) Nov. 23, 2012.
2. M.C. Billone, T.A. Burtseva, and R.E. Einziger, J. Nucl. Mater. 433, 431-448 (2013).
3. M.C. Billone, T.A. Burtseva, J.P. Dobrzynski, Z. Han, and Y.Y. Liu, *Effects of Multiple Drying Cycles on High-Burnup PWR Cladding Alloys*, FCRD-UFD-2014-000052, ANL-14/11, Sep. 26, 2014.
4. NRC 2003 Interim Staff Guidance (ISG)-11, Revision 3, "Cladding Considerations for the Transportation and Storage of Spent Fuel" (2003).
5. M.C. Billone, T.A. Burtseva, and Y.Y. Liu, "Effects of Drying and Storage on High-Burnup Cladding Ductility," Proc. IHLRWMC, Albuquerque, NM, April 28-May 2, 2013, Paper 6973, 1106 –1113 (2013).
6. J.J. Kearns, J. Nucl. Mater. *22*, 292-303 (1967).
7. B.F. Kammenzind, D.G. Franklin, H.R. Peters, and W.J. Duffin, "Hydrogen Pickup and Redistribution in Alpha-Annealed Zircaloy-4," *Zirconium in the Nuclear Industry: 11th Intl. Symp.*, ASTM STP 1295, E.R. Bradley and G.P. Sabol, Eds., ASTM, pp. 338-370 (1996).
8. A. McMinn, E.C. Darby, and J.S. Schofield, "The Terminal Solid Solubility of Hydrogen in Zirconium Alloys, *Zirconium in the Nuclear Industry: 12th Intl. Symp.*, ASTM STP 1354, G.P. Sabol and G.D. Moan, Eds., ASTM, pp. 173-195 (2000).
9. M.C. Billone, T.A. Burtseva, and Y. Yan, *Ductile-to-Brittle Transition Temperature for High-Burnup Zircaloy-4 and ZIRLO™ Cladding Alloys Exposed to Simulated Drying-Storage Conditions*, Argonne National Laboratory Report ANL-13/13, NRC ADAMS ML12181A238 (Sept. 2012).
10. M. Aomi, T. Baba, T. Miyashita, K. Kaminura, T. Yasuda, Y. Shinohara, and T. Takeda, J. ASTM Intl., JAl101262 (2008).